

Is Dual Linear Self-Calibration Artificially Ambiguous?

Pierre Gurdjos

ENSEEIH - IRIT, Toulouse, France

Adrien Bartoli

CNRS - LASMEA, Clermont-Ferrand, France

Peter Sturm

LJK - INRIA, Grenoble, France

Abstract

This purely theoretical work investigates the problem of artificial singularities in camera self-calibration. Self-calibration allows one to upgrade a projective reconstruction to metric and has a concise and well-understood formulation based on the Dual Absolute Quadric (DAQ), a rank-3 quadric envelope satisfying (nonlinear) ‘spectral constraints’: it must be positive of rank 3. The practical scenario we consider is the one of square pixels, known principal point and varying unknown focal length, for which generic Critical Motion Sequences (CMS) have been thoroughly derived. The standard linear self-calibration algorithm uses the DAQ paradigm but ignores the spectral constraints. It thus has artificial CMSs, which have barely been studied so far.

We propose an algebraic model of singularities based on the confocal quadric theory. It allows to easily derive all types of CMSs. We first review the already known generic CMSs, for which any self-calibration algorithm fails. We then describe all CMSs for the standard linear self-calibration algorithm; among those are artificial CMSs caused by the above spectral constraints being neglected. We then show how to detect CMSs. If this is the case it is actually possible to uniquely identify the correct self-calibration solution, based on a notion of signature of quadrics. The main conclusion of this paper is that a posteriori enforcing the spectral constraints in linear self-calibration is discriminant enough to resolve all artificial CMSs.

1. Introduction

Structure-from-Motion (SfM) is the problem of recovering a metric model—the scene structure and the camera motion and intrinsic parameters—from multiple views. It has been extensively studied over the past few decades (see *e.g.* [5, 8]). The self-calibration paradigm allows one to solve SfM with few assumptions about the intrinsics and barely none about the structure and the motion, thus making SfM versatile and flexible. In theory, the mere zero-skew assumption is sufficient for the SfM problem to be well-posed [9]. We make the stronger standard assumption that

the pixels are square and the principal point lies at the image centre, but that the focal length is time-varying.

One of the most remarkable results in SfM says that, given enough point correspondences, a projective reconstruction of 3D points and cameras can be computed [6, 4, 7]. The metric upgrade of this model is a further reconstruction step, that draws on the equivalence of the projective to the metric model via an unknown 3D homography. This is mathematically formulated using the elegant geometrical paradigm of the Dual Absolute Quadric (DAQ) proposed by Triggs in 1997 [22], which has also been extended to that of the Absolute Quadratic Complex [13, 23]. The DAQ has nonlinear ‘spectral constraints’: it is semi-positive and rank-3. This models the fact that the DAQ is the plane-envelope of the Absolute Conic, a virtual conic (*i.e.* consisting only of complex points). Once the DAQ is recovered, the upgrading homography is easily extracted from it. This class of algorithms has been popularised by the linear least-squares formulation of Pollefeys *et al.* [12, 17], which is hereafter dubbed *dual linear self-calibration*. Recently, self-calibration approaches enforcing the spectral constraints while globally optimizing some algebraic error measure have been proposed [2, 3]. However, the above dual linear self-calibration approach is probably still the most used one.

As mentioned in [8, p498], ‘*self-calibration can work well in the right circumstances, but used recklessly it will fail*’, especially if one does not ‘*take care to avoid ambiguous motion sequences*’, so-called *critical motion sequences (CMSs)*. For these, there exist more than one virtual conic satisfying the self-calibration constraints. Sturm [21] and Kahl *et al.* [10] studied this problem and established that there exist *generic* critical motion sequences for the camera, and that they defeat any self-calibration algorithm.

The SfM framework has all its basic building blocks in place. There is however an important missing piece regarding *artificial CMSs*. It has been known that there exist CMSs which are not generic for the self-calibration problem, but for which the dual linear self-calibration algorithm fails in finding the ‘true’ DAQ [20]. This is essentially due to this algorithm ignoring the spectral constraints. In other words, in generic criticality, only quadric envelopes

representing a virtual conic can satisfy the self-calibration equations while, in artificial criticality, any quadric envelope (virtual or not, degenerate or not) can satisfy them. In the case where a linear self-calibration algorithm returns a 1D family of ambiguous solutions, previous works [12, 17] showed that the rank-deficiency constraint can be enforced *a posteriori* to select candidate solutions. Bartoli *et al.* [1] select the most realistic solution by examining the camera focal length.

In this paper, we propose a theoretical framework for exhaustively studying CMSs in dual linear self-calibration, based on the *confocal quadric theory*. Interestingly enough, this theory has been established long ago by famous mathematicians. The resulting framework can be viewed as an add-on to the DAQ model of self-calibration. The main conclusion of this paper is thus that for the studied self-calibration problem, even linear algorithms only suffer from the generic CMSs, if spectral constraints are enforced *a posteriori*.

Paper organization. In section 2, the self-calibration problem and its ingredients are formulated and the notion of CMS is defined. Generic CMSs are reviewed in section 3. In section 4, we provide an exhaustive list of CMSs for dual linear self-calibration and highlight which of these are artificial, *i.e.* only exist due to neglecting the spectral constraints. Some details on the underlying theoretical analysis are provided in section 5. In section 6, we show how a projectively invariant signature for quadrics allows one to identify the type of CMS that caused linear self-calibration to give ambiguous results. Finally, we explain that in the case of an artificial CMS, this signature allows us to uniquely recover the true self-calibration solution.

2. Problem Formulation

We consider the self-calibration problem for the case of a varying focal length but where the other intrinsic parameters are known. Let us review the classical formulation based on the *Dual Absolute Quadric* (DAQ) [22]. This is the plane-envelope of the *Absolute Conic* Ω_∞ (AC). Given a 3×4 perspective projection matrix P , the image of the DAQ is given by the projection equation

$$\omega^* \sim PQ_\infty^* P^\top. \quad (1)$$

where ω^* is the *Dual Image of the Absolute Conic* (DIAC).

We assume to be given a set of n cameras obtained by means of projective reconstruction, that we write

$$P^j = \begin{pmatrix} \mathbf{a}^{j\top} \\ \mathbf{b}^{j\top} \\ \mathbf{c}^{j\top} \end{pmatrix}, \quad j = 1, \dots, n \quad (2)$$

where \mathbf{a}^j , \mathbf{b}^j and \mathbf{c}^j are 4-vectors representing planes.

Camera j projects the DAQ to ω^{*j} . Under the above assumptions on the camera's intrinsic parameters, we may assume $\omega^{*j} \sim \text{diag}((f^j)^2, (f^j)^2, 1)$, where f^j denotes the focal length of camera j . It can be readily seen that Q_∞^* then satisfies a set of four linear equations for each camera:

$$\begin{aligned} \mathbf{a}^{j\top} Q_\infty^* \mathbf{a}^j - \mathbf{b}^{j\top} Q_\infty^* \mathbf{b}^j &= 0, & \mathbf{a}^{j\top} Q_\infty^* \mathbf{b}^j &= 0, \\ \mathbf{a}^{j\top} Q_\infty^* \mathbf{c}^j &= 0, & \mathbf{b}^{j\top} Q_\infty^* \mathbf{c}^j &= 0. \end{aligned} \quad (3)$$

Solving those constraints for multiple cameras *e.g.*, by optimizing in a linear least squares manner forms the basis of the dual linear self-calibration algorithms [11].

Additional constraints are that the DAQ Q_∞^* has rank 3 and is positive semi-definite. These constraints are non-linear and are thus not taken into account in dual linear self-calibration.

In this paper, we investigate critical motion sequences (CMS) for self-calibration, *i.e.*, camera motions for which the problem does not have a unique solution. It is well known that there are CMSs that are generic for a given self-calibration problem, in the sense that any algorithm will suffer from them, and that some algorithms may suffer from additional, *artificial* CMSs, due to not exploiting all available constraints [20]. In this paper, we study this issue for dual linear self-calibration. In section 3, we first review the generic CMSs and in section 4 we then derive all CMSs for dual linear self-calibration and explain which among these are artificial. After that, we show how artificial CMSs can be detected from an ambiguous self-calibration result and that the ambiguity can indeed be resolved.

The definition of a CMS is as follows. Let the true cameras be $P_E^j \sim \text{diag}(f^j, f^j, 1)R^j \begin{pmatrix} \mathbf{I} & | & -\mathbf{t}^j \end{pmatrix}$. If there exists a Q^* different from the true DAQ that satisfies all self-calibration constraints (equations (3,4) as well as the (spectral) rank-3 and positiveness constraints on Q_∞^*), then the set of camera poses is termed a generic CMS. Artificial CMS for dual linear self-calibration are additional sets of camera poses for which there exists a Q^* different from the true DAQ that only satisfies the linear equations (3,4). In these cases, Q^* is called a '*false DAQ*'.

3. Generic Critical Motion Sequences

The generic CMSs for self-calibration with varying focal length have been derived by Sturm [21] and Kahl *et al.* [10]. They proceeded as follows. They sought after virtual proper conics in 'regular' 3-space (in contrast to a search in 'dual' 3-space) other than the AC; if such a conic exists that satisfies all constraints, it is called a 'false' AC. With regard to their approach, the self-calibration equations (3,4) have a simple meaning: they impose that the image of the AC is a circle, centered in the principal point. The image of a conic is such a circle, exactly if the cone, with centre the camera's optical centre and containing the conic, is a right (circular)

cone. This geometric interpretation of the self-calibration constraints can now be used to reason on critical motions. Consider the existence of a false AC. Then, any camera *position* in a CMS, must satisfy the constraint that the cone, with centre the optical center and tangent to the false AC, is circular. Further, for any such camera position, the camera *orientation* must be such that the optical axis coincides with a revolution axis of that cone.

Based on this interpretation, Sturm and Kahl *et al.* derived all types of critical motions. This was done by considering all possible cases of false ACs and working out the camera positions and orientations according to the above definition. Basically Sturm and Kahl *et al.* (re)discovered (and proved) a specialised case of the following result: *the locus of the vertices of a circular cone through a conic consists of its conjugate conics*, which is illustrated in Fig. 1. By definition, two *conjugate conics* are conics lying on perpendicular planes and having an axis in common and the foci-pair (either both real or complex conjugate) of one conic must be coinciding with the intersection point-pair of the other with this axis [18, p245]. We wrote ‘rediscovered’ as this more general result has been known for a long time and is attributed to Dupin and Steiner in [19, p82].

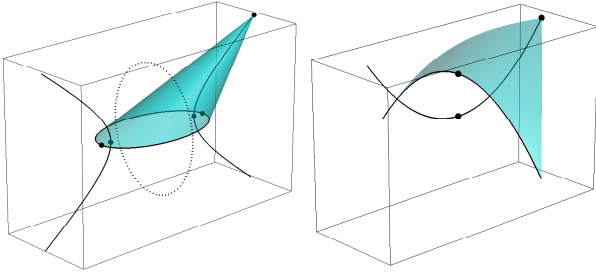


Figure 1. The two types of focal conic-sets: (left) ellipse / hyperbola / virtual-conic triplet; (right) parabola / parabola pair. Focal conics have the remarkable general property of being *conjugate* (see text) and each conic completely determines the others.

4. Artificial Critical Motion Sequences

We now consider dual *linear* self-calibration *i.e.*, the problem of estimating the DAQ without imposing that it is rank 3 and positive semi-definite *i.e.*, without imposing that the AC is actually a conic and that it is a *virtual* conic. In other words, any quadric in dual form can now be a candidate false DAQ, under the condition that it satisfies the constraints expressed in (3,4). As explained above, these convey exactly that the image of the DAQ is a circle centered in the image’s principal point (to be precise, the dual of such a circle). A set of camera poses is thus critical if there exists another dual quadric that is projected to centered circles in all images. More exactly, the existence of such a CMS

is equivalent to that of a p -parameter *linear* family of false DAQs with $p > 0$. Terminology-wise, a CMS is said to be *degenerate* if the solution family is entirely degenerate *i.e.*, if it consists of ∞^p *degenerate* dual quadrics D^* . It is not proved here but a condition for this is that D^* is ‘squashed’ at infinity *i.e.*, its points are located on the plane at infinity π_∞ *i.e.*, $D^* \pi_\infty = \mathbf{0}_4$.

Consider now a dual quadric and a cone enveloping it whose vertex is the optical center. Its image is a centered circle (radii can be zero or imaginary) exactly if that cone is circular and if the camera’s optical axis is aligned with a revolution axis of the cone. Based on this observation, CMS can be derived as in the works cited in the previous section, by considering all (Euclidean) types of dual quadrics, and determining the camera poses that satisfy the above constraints. This latter task is greatly simplified due to results in the projective geometry literature of the 19th- and the early 20th-century [15, 18, 19]. In the following, we briefly summarize these and their implications for our study.

Before going further let us introduce the notions of (real and imaginary) foci and focal axes of a quadric (*e.g.*, as in [16, p339] or [18, p225]). Any point such that the tangent-cone to a quadric with that point as vertex, is circular, is a **focus** of the quadric. Any line through a focus relative to which that cone is rotationally symmetric is a **focal axis** of the quadric. This is illustrated in Fig. 2. Note that for each focus, there is either a single focal axis, or all lines through it are focal axes (this is the case if the mentioned cone is isotropic *i.e.*, contains the AC).

Regarding the issue of which dual quadrics other than the DAQ, get projected to a dual circle that is centred in the principal point, the answer is surprisingly enough quite simple: these are the quadrics for which the camera centre is a real focus and the optical axis a real focal axis. The result that we infer from this is fundamental; a sketch of the proof is given in the appendix.

Prop. 1 (Fundamental condition) *A motion sequence is critical iff there exists an irreducible¹ quadric other than the DAQ such that:*

1. any camera centre is a focus of the quadric,
2. any optical axis is a focal axis of the quadric.

In other words, it is equivalent to say that a camera motion is critical or that the camera moves on the ‘focal curve’ of some irreducible quadric while its optical axis, for each position, is a focal axis of the quadric through the camera centre. Note that, as a result, *only the orientation of the camera’s optical axis matters*, whereas rotation about the optical axis is irrelevant.

What are the foci of a quadric? A first main classical result we use has been established long ago: a **focus of a**

¹A (full) rank-4 or (deficient) rank-3 quadric in locus or envelope form.

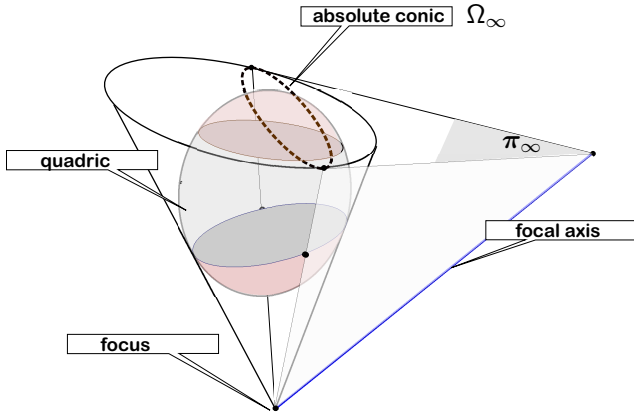


Figure 2. A focus and a focal axis of a quadric respectively coincide with the vertex and the revolution axis of a circular cone (*i.e.*, having double contact with Ω_∞) enveloping the quadric (see text).

quadric is a point of its **focal conics** (a set of focal curves also called **focals**, *cf.* [19, p81]) which are conics lying on its principal planes (mutually orthogonal and such that any two of them share a principal axis). There are other properties, see *e.g.* [18]. Furthermore, it is known that there are *only two* types of focal conic-sets of a general quadric²: (i) the parabola/parabola pair, (ii) the ellipse/hyperbola/virtual conic triplet (see Fig. 1). Other quadrics need special treatments that will be discussed in the sequel.

The second main result is due to Chasles (see [19, p81] and also [14]). It describes how to obtain the focal conics of a general quadric Q . Consider the **confocal range** of its dual Q^* , *i.e.* the 1D linear family of dual quadrics spanned by Q^* and the DAQ Q_∞^* . This family has in general four degenerate members; these, except Q_∞^* , are exactly the envelopes of the focal conics of Q .

What are the focal axes of a quadric? A **focal axis** of a quadric is a line through which the two (complex) planes touching the AC are also tangent to the quadric [18, p224] (see Fig. 2). Thanks in particular to Plücker (see [19, p82]), it has been established that *the assemblage of focal axes of a quadric consists of the generators i.e., the axes of pencils of planes*, of the quadrics of its confocal range. The general notion of focal axis is less intuitive than that of focus and, as we are only interested in focal axes through foci, we will not look deeper into the theory of confocal quadrics.

5. The Geometry of Criticality

The above results, in particular Chasles' result, can be used to efficiently derive types of CMSs as shown in the following section. To determine all possible geometries of CMSs, it now suffices to compute the focal conics of quadrics of different Euclidean types and to describe the results

²Here, a general quadric is a proper quadric that is not of revolution.

in a generic geometric manner (this is done quite easily using a symbolic software like MAPLE). It is rather mechanical to carry out this procedure (see *e.g.*, example 2 below), besides a few exceptions explained below (*e.g.*, example 3). The results are summarized in table 1, which contains all critical motions for the dual linear self-calibration problem.

To obtain these results, we needed to consider, besides the above classical geometric results, several other issues. First, these results only directly provide the camera *positions* in a CMS, the camera *orientations* are less directly given and are obtained algebraically. Second, as said previously, these results only hold for general proper quadrics; the cases of quadrics of revolution, spheres, and degenerate quadrics, need special treatment.

If we deal with a quadric of revolution, there is a major specificity: one conic in its focal-set is repeated and degenerates into either a rank-1 or a 'rank-0' conic (see Fig. 3). Note that no rank-2 focal conic does exist. The rank-1 focal conic is a ('repeated') line that coincides with the axis of revolution of the quadric. We will also call this a **focal line**. It contains two specialised foci called **principal foci**, which are the two foci of the conic obtained by meridian-section³ of the quadric. In the special case of a sphere, this linear locus of foci further degenerates into a 'rank-0 conic', meaning that every point in 3-space is a focus of the sphere. The sphere has a single **principal focus**, its centre. Note that all lines passing through a principal focus, are focal axes of the quadric.

Let us consider, for these special cases, the nature of focal axes that pass through a focus (keep in mind that they determine the orientation of optical axes in CMSs). Consider first the general case of a quadric having general focal conics. For any point on such a focal conic, the focal axis passing through it coincides with the tangent line to that focal conic at that point which is coplanar with the focal conic. Next, we consider the case of a focal line, which happens for quadrics of revolution, see above. For any point on a focal line, the focal axis passing through that point is the focal line itself (which is always a real line). An exception are the two principal foci, where any line passing through them is a focal axis. Finally, in the case of a sphere, every point in 3-space is a focus, as explained above, and through it there is just one focal axis which is the line joining that point and the centre of the sphere. Again, an exception is the centre of the sphere itself, for which all lines passing through it, are focal axes (see Fig. 3).

There are two classes of confocal ranges for which the locus of foci is the entire 3-space *i.e.*, a focal space. The first includes (i) all confocal (*i.e.*, concentric) ranges of spheres (type (R4) in table 1) and the second (ii) all degenerate confocal ranges, for which arbitrary values of α_1, α_2 satisfy $\det(\alpha_1 Q^* + \alpha_2 Q_\infty^*) = 0$ (type (D)). Here, degenerate con-

³Any planar section of the quadric through its axis of revolution.

focal quadric ranges correspond to ranges of conics at infinity with the dual absolute conic Ω_∞^* as member (cf. § 4). What distinguishes (i) and (ii) is that, in the former case, the focal axes through foci concur at a finite (unique) principal focus; in the latter case, they concur at a principal foci at infinity and hence all focal axes are parallel.

We now give two examples carrying some technical details on how to determine the real points of the focal conics. Other cases are solved in very similar ways.

Example 2 We here determine the foci and focal axes of a central quadric Q (class G1). Write the envelope of Q in Euclidean canonical form as

$$Q^* = \text{diag}(a_1, a_2, a_3, -1)$$

The parameters of the degenerate envelopes of the confocal range determined by Q^* are the generalized eigenvalues of the matrix-pair (Q^*, Q_∞^*) which can be easily computed since $Q_\infty^* = \text{diag}(1, 1, 1, 0)$. These parameters are a_1, a_2, a_3 and ∞ (the latter is the parameter of Q_∞^*). Hence it is straightforward to compute, in this order, the matrices of the degenerate envelopes —other than Q_∞^* — and their (ordinary) eigenvalues:

$$F_1^* = \begin{pmatrix} 0 & 0 & 0 & 0 \\ 0 & a_2 - a_1 & 0 & 0 \\ 0 & 0 & a_3 - a_1 & 0 \\ 0 & 0 & 0 & -1 \end{pmatrix}; \text{eig}(F_1^*) = \begin{pmatrix} 0 \\ -1 \\ a_3 - a_1 \\ a_2 - a_1 \end{pmatrix}$$

$$F_2^* = \begin{pmatrix} a_1 - a_2 & 0 & 0 & 0 \\ 0 & 0 & 0 & 0 \\ 0 & 0 & a_3 - a_2 & 0 \\ 0 & 0 & 0 & -1 \end{pmatrix}; \text{eig}(F_2^*) = \begin{pmatrix} 0 \\ -1 \\ a_3 - a_2 \\ a_1 - a_2 \end{pmatrix}$$

$$F_3^* = \begin{pmatrix} a_1 - a_3 & 0 & 0 & 0 \\ 0 & a_2 - a_3 & 0 & 0 \\ 0 & 0 & 0 & 0 \\ 0 & 0 & 0 & -1 \end{pmatrix}; \text{eig}(F_3^*) = \begin{pmatrix} 0 \\ -1 \\ a_2 - a_3 \\ a_1 - a_3 \end{pmatrix}$$

The F_k^* 's are matrices of three rank-3 dual quadrics encoding three focal conics on the principal planes of the quadric (point-equations of these focals can be easily derived). Assume Q to be general e.g., $a_1 < a_2 < a_3$ and $a_1 a_2 a_3 \neq 0$. The first two point-equations represent conjugate focal conics i.e., a (real) ellipse on the YZ -plane and a (real) hyperbola on the XZ -plane respectively, while the third one represents a virtual ellipse on the XY -plane. Each tangent line to the conic on the supporting plane of the conic is the axis of a pencil of planes of F_k^* and thus is a focal axis of Q .

Example 3 We now determine the foci and focal axes of an elliptic paraboloid of revolution Q (R3). Write the envelope of Q in Euclidean canonical form as

$$Q^* = \begin{pmatrix} 1 & 0 & 0 & 0 \\ 0 & 1 & 0 & 0 \\ 0 & 0 & 0 & 2/b \\ 0 & 0 & 2/b & 0 \end{pmatrix} \quad b \neq 0. \quad (5)$$

The parameters of the degenerate envelopes of the confocal range of Q^* are the generalized eigenvalues of (Q^*, Q_∞^*) . One gets generalized eigenvalues equal to 1 and ∞ , both with multiplicity two (∞ is the parameter of Q_∞^*). The matrix of the single 'focal' degenerate envelope (with parameter 1) is given below with its (ordinary) eigenvalues:

$$F^* = \begin{pmatrix} 0 & 0 & 0 & 0 \\ 0 & 0 & 0 & 0 \\ 0 & 0 & -1 & 2/b \\ 0 & 0 & 2/b & 0 \end{pmatrix}; \quad \text{eig}(F^*) = \frac{1}{2b} \begin{pmatrix} 0 \\ 0 \\ -b + (b^2 + 16)^{1/2} \\ -b - (b^2 + 16)^{1/2} \end{pmatrix}$$

As the product of the 3rd and 4th eigenvalues yields $-4/b^2$, one deduces that F^* is a real point-pair, say $F^* = \mathbf{f}\mathbf{g}^\top + \mathbf{g}\mathbf{f}^\top$ where $\mathbf{f}, \mathbf{g} \in \mathbb{R}^4$, formed by the two principal foci of the quadric. By inspecting the element $F_{44}^* = 0 = 2f_4g_4$, one can see that \mathbf{f} or \mathbf{g} —but not both— is at infinity. The line spanned by \mathbf{f} and \mathbf{g} is a focal line i.e., a rank-1 focal conic. Through each of \mathbf{f} and \mathbf{g} , there passes ∞^2 planes (a star of planes) and hence ∞^2 lines which are the focal axes of Q , including the line through \mathbf{f} and \mathbf{g} .

Along these lines, we can derive all CMSs; they are summarized in table 1. Naturally, they subsume the generic critical motions summarized in section 3. Concretely, the classes of motions (G1), (R1) and (D) are generic critical motions, all others are artificial ones for the dual linear self-calibration approach (see Fig. 4).

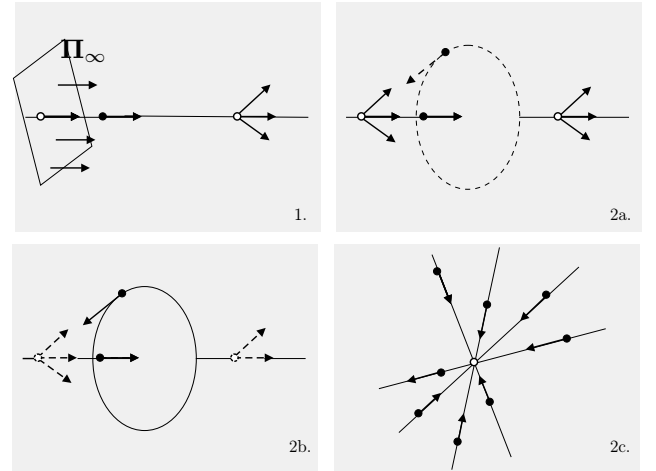


Figure 3. Four degenerate types of focus loci (black dots), including principal foci (white dots), and assemblage of focal axes through them (arrows). The dashed style indicates virtual objects. The general case is shown in Fig. 1.

6. How to Detect Artificial Critical Motions

In this section, we show how one may detect and handle artificial CMSs, starting from a projective reconstruction.

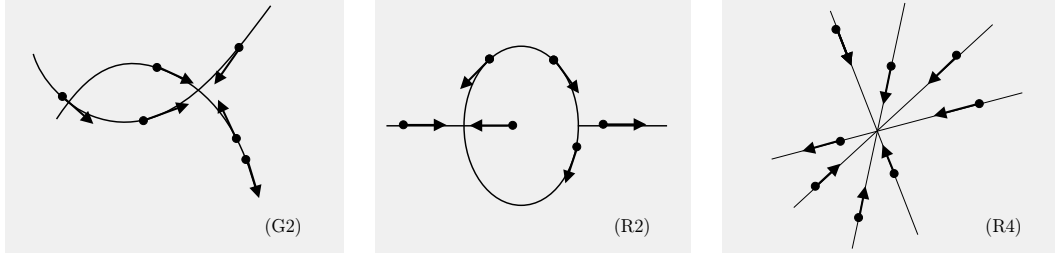


Figure 4. The three classes (G2), (R2) and (R4) of artificial CMS completing the known generic CMS. The ambiguity for the DAQ is 1D if the CMS is rank-2 *i.e.*, it includes at least three cameras with at least one on the circle for (R2).

Quadric Confocal Ranges	Degenerate envelopes (focal conics) and associated signature sequence	Critical motions: locus \mathcal{L} of camera centres and associated assemblage \mathcal{A} of optical axes.
(G1) General virtual ellipsoids, ellipsoids and hyperboloids of one or two sheets	$\{ Q_{\infty}^*, Q_{\text{virt}}^*, E^*, H^* \}$ $\{ (3, 0), (3, 0), (2, 1), (2, 1) \}$	\mathcal{L} is a conjugate conic-pair formed by a general ellipse and a general hyperbola; \mathcal{A} consists of axes tangent to these conics in their supporting planes.
(G2) General elliptic and hyperbolic paraboloids	$\{ Q_{\infty}^* \times 2, P_1^*, P_2^* \}$ $\{ ((3, 0)), (2, 1), (2, 1) \}$	\mathcal{L} is a conjugate conic-pair formed by two general parabolas; \mathcal{A} consists of axes tangent to these conics in their supporting planes.
(R1) Prolate ellipsoids and hyperboloids of two sheets, oblate virtual ellipsoids	$\{ Q_{\infty}^*, C_{\text{virt}}^*, (\mathbf{F}\mathbf{F}'^{\top} + \mathbf{F}'\mathbf{F}^{\top}) \times 2 \}$ $\{ (3, 0), (3, 0), ((1, 1)) \}$	\mathcal{L} is a single line; \mathcal{A} consists of \mathcal{L} and two stars of axes through two fixed finite points on \mathcal{L} .
(R2) oblate ellipsoids and hyperboloids of one sheet; prolate virtual ellipsoids	$\{ Q_{\infty}^*, C^*, (\mathbf{F}_+\mathbf{F}_+^{\top} + \mathbf{F}_-\mathbf{F}_-^{\top}) \times 2 \}$ $\{ (3, 0), (2, 1), ((2, 0)) \}$	\mathcal{L} consists of a circle and a line which cuts orthogonally its centre; \mathcal{A} consists of this line and the axes tangent to the circle in its supporting plane.
(R3) Elliptic paraboloids of revolution	$\{ Q_{\infty}^* \times 2, (\mathbf{F}\mathbf{F}'^{\top} + \mathbf{F}'\mathbf{F}^{\top}) \times 2 \}$ $\{ ((3, 0)), ((1, 1)) \}$	\mathcal{L} is a single line; \mathcal{A} consists of two stars of axes through two fixed points on \mathcal{L} , one finite and the other infinite.
(R4) Spheres	$\{ Q_{\infty}^*, \mathbf{C}\mathbf{C}^{\top} \times 3 \}$ $\{ (3, 0), (((1, 0))) \}$	\mathcal{L} is the 3-space; \mathcal{A} consists of a star of nonparallel axes, through a fixed finite point.
(D) Degenerate confocal ranges	∞^1 degenerate envelopes	\mathcal{L} is the 3-space; \mathcal{A} consists of all parallel axes.

Table 1. *All types of critical motions, induced by a seven-class partition of confocal ranges* w.r.t. signature sequences. Glossary: virtual degenerate envelopes are marked by ‘virt’ – objects at infinity are marked by ‘ ∞ ’. E_{virt}^* : virtual ellipse, E^* : ellipse, H^* : hyperbola, P_j^* : parabola j , C^* : circle, $(\mathbf{F}, \mathbf{F}')$: (real) principal foci-pair, $(\mathbf{F}_+, \mathbf{F}_-)$: (complex conjugate) principal foci-pair, \mathbf{C} : single principal focus.

This is based on the notion of *signature* of a degenerate dual quadric D^* .

Let ρ and ν be respectively the numbers of positive and negative eigenvalues of D^* . The signature of D^* is the pair (ξ_1, ξ_2) with $\xi_1 \equiv \max(\rho, \nu)$ and $\xi_2 \equiv \min(\rho, \nu)$ while $\xi_1 + \xi_2 = \text{rank } D^*$. A crucial property of signature and rank is that they are *invariant to homographies* [8, p74].

A projective description of a confocal range, spanned by

Q_1^* and Q_2^* , is now given by its *signature sequence*

$$\{ (\dots (\xi_1^1, \xi_2^1) \dots), \dots, (\dots (\xi_1^r, \xi_2^r) \dots) \} \quad (6)$$

where $r \in \{1..4\}$ and

- (ξ_1^r, ξ_2^r) is the signature of any degenerate $Q_1^* - \lambda_r Q_2^*$, where λ_r is a generalized eigenvalue of (Q_1^*, Q_2^*) ;
- the number of brackets around a signature (*cf.* 2nd column of table 1) indicates the number of times that $Q_1^* - \lambda_r Q_2^*$ is repeated in the set of degenerate envel-

opes *i.e.*, the algebraic eigenvalue multiplicity of λ_r .

The signature sequence describes the four (possibly repeated) degenerate dual quadrics of the range. It yields a *projective description* as it relies on signatures and multiplicities of these dual quadrics which are the same in any projective representation⁴.

The signature sequences including the signatures of the false DAQs for all cases of CMSs, are given in table 1. They are at the basis of identifying and handling artificial CMSs, as described in the following.

Let us consider the solution of the linear self-calibration equations (3,4). Of course, if there are ambiguous solutions, we are in the presence of a critical motion. Since we deal with linear equations, ambiguous solutions correspond to a linear family of dual quadrics. We assume that there is only a 1D linear family. This is the most practical common case as soon as there are $n \geq 3$ critical cameras taken anywhere in the critical sequence⁵, except for (R2) in which at least one must be on the circle, cf. Fig. 4. This can be easily proved *e.g.*, using MAPLE. We first compute the four degenerate members of that linear family, *e.g.* by computing the generalized eigenvalues of a pair of dual quadrics that span the family. Then, for each of these degenerate dual quadrics, we compute its signature. A first observation is that the signature sequence allows one to uniquely identify the class of CMSs (*cf.* 2nd column of table 1). A second observation is that all false DAQs of all artificial critical motions (classes (G2), (R2), (R3) and (R4)) have a signature that is different from that of the true DAQ, (3, 0). Hence, in the presence of an artificial CMSs, the true DAQ can be identified without ambiguity, as the single one having signature (3, 0). In conclusion, artificial CMSs can, when taking into account all self-calibration constraints after solving the linear equation system, always be disambiguated. Figure 5 shows a typical example where our algorithm resolves an artificial CMS.

7. Conclusions

Our theoretical results have two major consequences in practical applications. First, existing SfM implementations using dual linear self-calibration [11, 12, 17] are known to be unstable due to degeneracies and noise. But degeneracies are intrinsically due to critical motions. Knowing the artificial CMSs will allow one to avoid them. Second, encapsulating the spectral constraints in the signature sequence, we proved that those are discriminant enough to find the true DAQ within a 1D family of potential DAQs. In other words, we stated that the spectral constraints can be safely enforced *a posteriori*, making it possible to avoid ambiguous self-calibration in the presence of artificial CMSs (refer

⁴A signature is projectively invariant by Sylvester’s law of inertia. The multiplicity of a generalized eigenvalue also has this property.

⁵We do not consider the class (D) here.

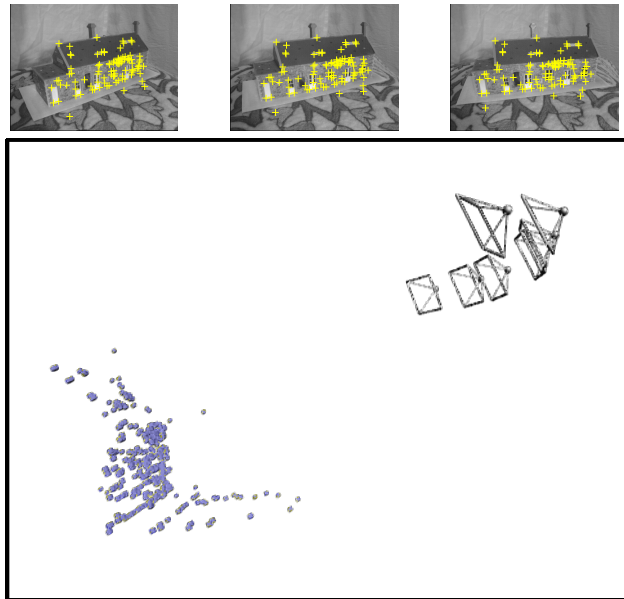


Figure 5. (3D interactive graphic) We ran the dual self-calibration linear algorithm from the publicly available “Model House” image sequence (www.robots.ox.ac.uk/vgg/data). To get the projective cameras, we used Sturm-Triggs’ projective factorization (see [8, p444]), followed by projective bundle adjustment. Only the first six (out of seven) frames were considered, forming a subsequence in which 94 2D points were matched all over. Regarding the self-calibration solution given by a SVD-based algorithm (similar to A5.3 in [8, p592]), after computing the ratios of the first singular value to the last three ones, respectively equal to $5.70e + 004$, $9.43e + 002$ and 32.83 , we concluded that we were facing a critical motion, which was confirmed by visualising the ‘meaningless’ 3D metric reconstruction associated with the lowest singular value. Hence, the solution for the DAQ is included in a tangential pencil of quadrics $\alpha_1 Q_1^* + \alpha_2 Q_2^*$. We normalise the Q_i^* ’s by dividing them by their largest singular values, and next assume that, regarding the signatures of the degenerate quadrics $Q_1^* - \lambda_r Q_2^*$ where the λ_r ’s are the generalized eigenvalues of (Q_1^*, Q_2^*) , any value lower than $10e - 3$ is zero. The obtained signature sequence (with no other ‘numerical trick’) was $\{(3,0),((1,0))\}$. This indicates that all the cameras fixates a point, whose matrix is associated with the signature corresponding to (1, 0). We picked up as solution the degenerate envelope associated with (3, 0) and obtained the reconstruction of points and cameras which is displayed here, completed by reconstructions of additional pair-wise matched points.

to the *interactive graphic* in Fig. 5).

References

- [1] A. Bartoli and P. Sturm. The 3D line motion matrix and alignment of line reconstructions. *IJCV*, 57(3):159–178, 2004.
- [2] B. Bocquillon, A. Bartoli, P. Gurdjos, and A. Crouzil. On constant focal length self-calibration from multiple views. In *CVPR*, 2007.

- [3] M. Chandraker, S. Agarwal, D. Kriegman, and S. Belongie. Globally optimal affine and metric upgrades in stratified autocalibration. In *ICCV*, 2007.
- [4] O. Faugeras. What can be seen in three dimensions with an uncalibrated stereo rig? In *ECCV*, 1992.
- [5] O. Faugeras, Q. Luong, and T. Papadopoulou. *The geometry of multiple images*. MIT Press, 2001.
- [6] S. Finsterwalder. Die geometrischen Grundlagen der Photogrammetrie. *Jahresbericht Deutscher Mathematik*, 6:1–44, 1899.
- [7] R. Hartley, R. Gupta, and T. Chang. Stereo from uncalibrated cameras. In *CVPR*, pages 761–764, 1992.
- [8] R. Hartley and A. Zisserman. *Multiple view geometry in computer vision*. Cambridge Univ. Press, 2003.
- [9] A. Heyden and K. Åström. Minimal conditions on intrinsic parameters for Euclidean reconstruction. In *ACCV*, 1997.
- [10] F. Kahl, B. Triggs, and K. Åström. Critical motions for auto-calibration when some intrinsic parameters can vary. *JMIV*, 13(2):131–146, 2000.
- [11] M. Pollefeys. Self-calibration and metric 3D reconstruction from uncalibrated image sequences. Ph.D. Thesis, ESAT-PSI, K.U.Leuven, 1999.
- [12] M. Pollefeys, R. Koch, and L. Van Gool. Self-calibration and metric reconstruction inspite of varying and unknown intrinsic camera parameters. *IJCV*, 32(1):7–25, 1999.
- [13] J. Ponce, K. McHenry, T. Papadopoulou, M. Teillaud, and B. Triggs. On the absolute quadratic complex and its application to autocalibration. In *CVPR*, volume 1, 2005.
- [14] E. Primrose. Foci of a quadric. *The Mathematical Gazette*, 40(332):135–136, may 1956.
- [15] G. Salmon. *A treatise on the analytic geometry of three dimensions*, volume 1 of 4th edition. Dublin, Hodges, Figgis, & Co, 1882.
- [16] J. Semple and G. Kneebone. *Algebraic projective geometry*. Oxford University Press, 1952.
- [17] Y. Seo and A. Heyden. Auto-calibration by linear iteration using the DAC equation. *IVC*, 22(11):919 – 926, 2004.
- [18] D. Sommerville. *Analytical geometry of three dimensions*. Cambridge University Press, 1939.
- [19] O. Staude and A. Grévy. Géométrie algébrique dans l’espace. In J. Molk, editor, *Encyclopédie des Sciences Mathématiques Pures et Appliquées*, volume III, chapter 4, pages 1–164. Jacques Gaby, 1992 edition, 1904–1916.
- [20] P. Sturm. A case against Kruppa’s equations for camera self-calibration. *PAMI*, 22(10):1199–1204, september 2000.
- [21] P. Sturm. Critical motion sequences for the self-calibration of cameras and stereo systems with variable focal length. *IVC*, 20(5-6):415–426, march 2002.
- [22] B. Triggs. Autocalibration and the absolute quadric. In *CVPR*, 1997.
- [23] A. Valdés and J. Ignacio Ronda. Camera autocalibration and the calibration pencil. *JMIV*, 23(2):167–174, 2005.

Appendix

Due to lack of space, only a sketch of the proof of proposition 1 can be given here. Before, we remind some

known projective facts [15, 16, 18]. Except for the plane at infinity π_∞ , which is real, all the planes of the DAQ Q_∞^* are complex conjugate; hence all the tangent-lines⁶ of Q_∞^* are also complex conjugate. We refer to such pairs as *isotropic plane-pairs* and *isotropic line-pairs* respectively. An important property of an *isotropic plane-pair* is to be *invariant under rotations around its axis i.e.*, the intersection line of its two planes.

We also require an alternate definition of the focus of quadric, which can be found in [15, p127] and actually applies in dual 3-space for an algebraic surface of any order. ‘A focus is a point through which can be drawn two lines, each touching the surface and meeting the absolute conic, and such that the tangent plane to the surface through either also touches the absolute conic.’

Now, let us reveal the complex geometry of equations (3,4) by considering the algebraically equivalent pair:

$$(\mathbf{a}^j \pm i\mathbf{b}^j)^\top Q_\infty^* (\mathbf{a}^j \pm i\mathbf{b}^j) = 0, \quad (7)$$

$$\mathbf{c}^j \top Q_\infty^* (\mathbf{a}^j \pm i\mathbf{b}^j) = 0, \quad (8)$$

with $i^2 = -1$. Thus, we treat \mathbf{a}^j (resp. \mathbf{b}^j) in (2) as the real (resp. imaginary) part of a complex conjugate plane-pair. Since any camera P^j , cf. (2), satisfies equations (7,8), then (i) $\pi_\pm^j = \mathbf{a}^j \pm i\mathbf{b}^j$ is an *isotropic plane-pair* whose axis is the optical axis, (ii) the intersection of π_\pm^j and \mathbf{c}^j , denoted $\pi_\pm^j \wedge \mathbf{c}^j$, is an *isotropic line-pair* through the optical centre \mathbf{O}^j . Indeed, using (7), (i) holds by definition of an isotropic plane-pair. Using (7,8), (ii) also holds by definition as the intersection of two planes \mathbf{p} and \mathbf{q} is a tangent line of a quadric envelope X^* iff both equations⁷ $\mathbf{p}^\top X^* \mathbf{p} = 0$ and $\mathbf{p}^\top X^* \mathbf{q} = 0$ are satisfied [15, pp147-148].

That said the proof can be sketched: (i) A camera P^j of the form (2) is critical w.r.t. $X^* \not\cong Q_\infty^*$ iff (ii) P^j and X^* satisfy (7,8). Using a similar reasoning as above, an equivalent condition is that (iii) the isotropic plane-pair π_\pm^j is also a plane-pair of X^* and (iv) the isotropic line-pair $\pi_\pm^j \wedge \mathbf{c}^j$ is also a tangent line-pair⁶ of X^* . When this holds, the optical centre is a point through which there pass two isotropic lines tangent to X and such that the isotropic planes through the lines belong to X^* . By the alternate definition, the optical axis is a real focal axis of X and the optical centre is a real focus on the focal axis.

⁶What is the tangent line to a dual quadric? A *tangent line to a quadric locus* is a line which meets the quadric at two coinciding points. Through a line there are just two planes which belong to a dual quadric; this line is a *tangent line to the dual quadric* if the two planes coincide.

⁷ \mathbf{p} should be a plane of X^* while \mathbf{q} should not.